# Closed Loop operation of the Boost Converter

[1]A. Teja, [2]R. Sai Rushitha, [3]V. Ganesh, [4]Ch. Govinda, [5]T. Abhilash, [6]P.Jitendar

[1,2,3,4]Department of Electrical and Electronics Engineering
Aditya Engineering College, Surampalem, Andhra Pradesh
[5]Accendere Knowledge Management Services, [6]Department of Electrical and Electronics Engineering, MLR Institute of Technology, Hyderabad

Email: [1]tejaappikonda98@gmail.com, [2]rushitha.ravanala0456@gmail.com,
[3]veesamganesh1234@gmail.com, [4]ch.govinda@aec.edu.in
[5]abhilash.tripuathi@accendere.co.in, [6]jitendar13@gmail.com

***Abstract***— Boost converters are popularly been used in various applications. In some of the applications, its closed-loop control is desired to obtain the required output. This paper introduces the operation of boost converter and proposes a method of closed loop operation. A proportional-integral (P-I) control along with a hysteresis band is employed to perform the closed-loop operation of the boost converter. The P-I values are chosen based on trial and error method. Finally, the proposed technique is simulated in MATLAB/SIMULINK environment and the results are presented.

*Keywords— boost converter, P-I control, closed-loop*

## 1. Introduction

In the family of DC-DC converters, boost converters are very widely used [1-3]. A boost converter is defined as a power electronic circuit that step-up the DC voltage. The output voltage of a boost converter is always greater than the source voltage. The advantages of a comprehensive power converter design approach were demonstrated previously on a buck converter and a half-bridge converter [4-8]. The design allows one to identify a set of power converter design parameters which satisfies all design requirements and concurrently minimizes the converter weight and/or loss.

The proposed technique offers the benefits of closed-loop control in spite of open-loop control. This technique employs a fine-tuned P-I controller and hysteresis band to perform the closed-loop operation. This script is detailed as follows: II$^{nd}$ Section explores the operation of the boost-converter, and its operating modes, in Section III, the closed-loop modulation scheme is presented, in IV$^{th}$ Section, the simulation results justifying the closed-loop control are presented and V$^{th}$ Section, discusses the conclusion.

## 2. System Configuration

Fig. 1 shows the proposed closed-loop modulation scheme for the boost converter. The power circuit of the boost converter consists of a DC-source, boost inductor (LB), Active switch (SB), Diode (DB), Filter capacitor (Cf) and the load (RL) [9-10]. The boost converter operates in two modes which are discussed as follows:

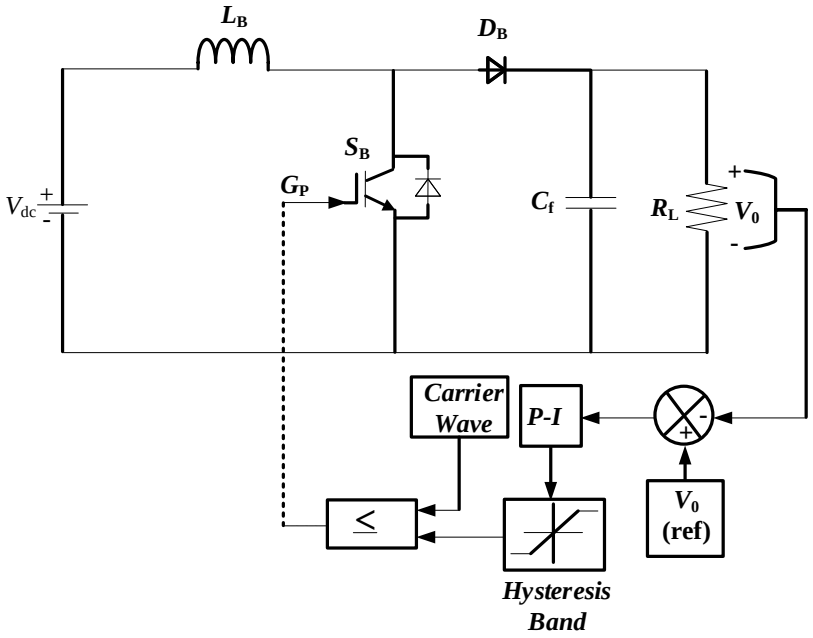


Fig. 1. Circuit diagram of the proposed configuration.

Mode-1: When the switch (SB) is on.
The equivalent circuit during mode-1 is shown in Fig. 2. During this mode, LB charges through the dc-supply and stores the energy in the form of magnetic field.

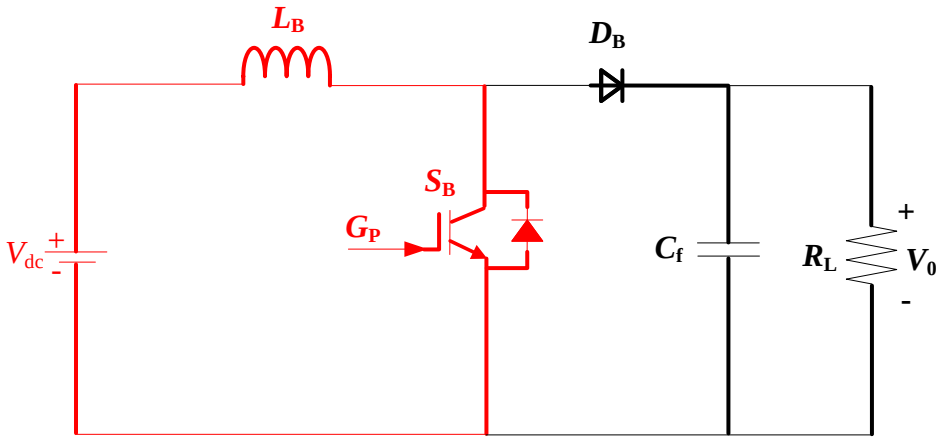


Fig. 2. Equivalent circuit during Mode-1.

Mode-2: When the switch (SB) is off.
The equivalent circuit during mode-2 is shown in Fig. 3. During this mode, the stored energy in the inductor (LB) discharges through the diode and to the load. In this mode both the voltage across the inductor and source voltage aids, due to which the average load voltage is greater than the source voltage. By applying the volt-sec balance in both the modes of operation, we obtain the relationship between output and input voltages as follows:

$$V_0 = \frac{V_{dc}}{1-D} \quad (1)$$

Where, D is the duty-ratio that is defined as the ratio of on-time to total-time.

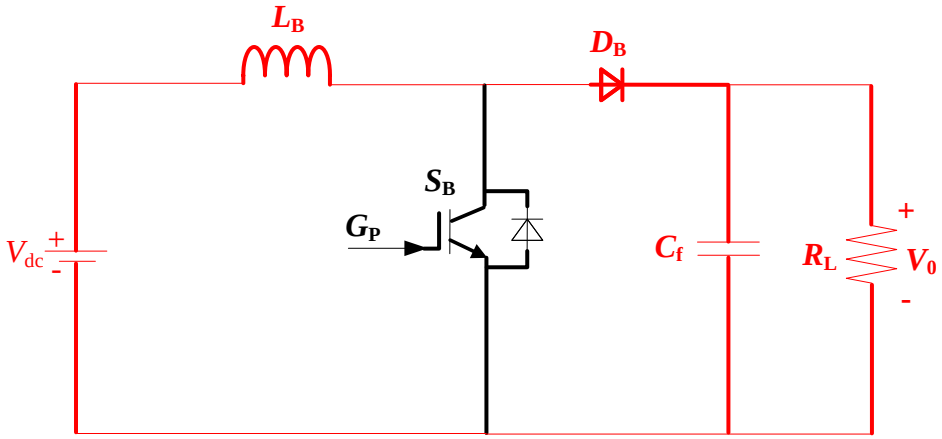


Fig. 3. Equivalent circuit during Mode-2.

### 3. Closed-loop Control Scheme

The closed-loop control scheme of the boost converter is shown in Fig. 1. Apart from the power circuit components, the logic diagram for closed-loop control is shown at the bottom of Fig. 1. It illustrates that the output voltage across the load is measured using a voltage sensor and the error signal is obtained by comparing it with the reference output voltage. The error signal is fed to a P-I control in which the values of P and I are selected by trail and error analysis. The output of the P-I controller is fed to hysteresis band, in which the upper and lower limits are set. Finally, the output of the hysteresis band circuit is compared with a carrier wave to generate the gate pulses to the boost converter active switch.

Table 1. Configuration Parameters

| Parameters | Values |
|---|---|
| $V_{dc}$ | (20-24) V |
| $L_B$ | 4.5 mH |
| $S_B$ | IGBT |
| $C_f$ | 1 mF |
| $R_L$ | 25 Ohm |

## 4. Simulation Results

The simulation parameters are considered to show both the steady-state and dynamic performance of the boost converter with the proposed technique. Table 1 gives the list of parameters considered for simulation studies. Figs. 4(a) and (b) shows the input voltage ($V_{dc}$), inductor current ($i_L$), and output voltage ($V_0$) waveforms of the boost converter for the reference output voltage ($V_0$ ref) 20 V and 24 V respectively. It can be seen that $V_{dc}$ is constant and ripple free. The ripple in the inductor current is slightly increasing when the reference output voltage is changed from 20 V to 24 V. In Fig. 4(a), the output voltage oscillates around the value of 20 V, whereas in Fig. 4(b), the output voltage oscillates around the value of 24 V. This shows the the proposed technique produces the output voltage in accordance with the reference command. The dynamic performance of the proposed method is evaluated by using a step-change in command. Fig. 5 illustrates the input and output voltages of the boost converter by a step-change in reference output voltage at t = 0.5 sec. It can be observed that, the initial output voltage is settled at an average value of 20 V from t = 0 to t = 0.5 sec. At t = 0.5 sec, due the application of change in reference output voltage, the output voltage jumps to an average value of 24 V in a short duration of time. Hence, the steady-state and dynamic performance of the boost converter with the proposed closed-loop control technique are evaluated.

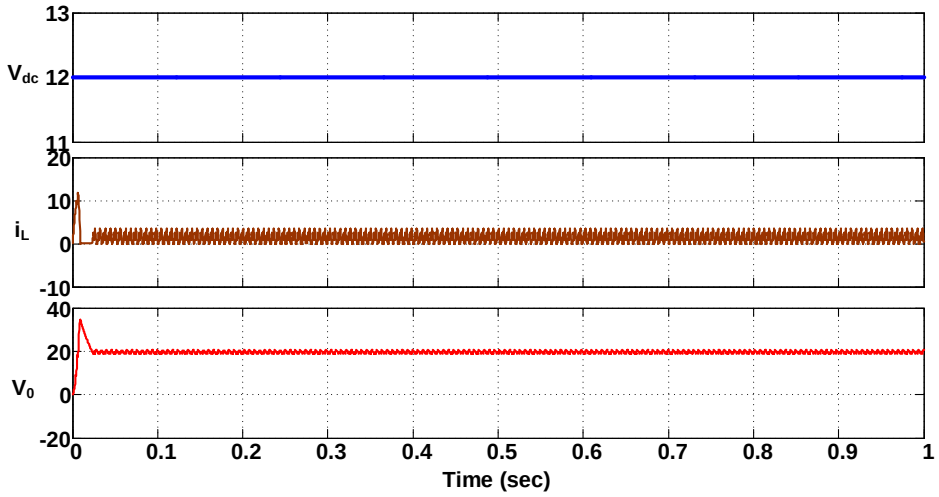


(a)

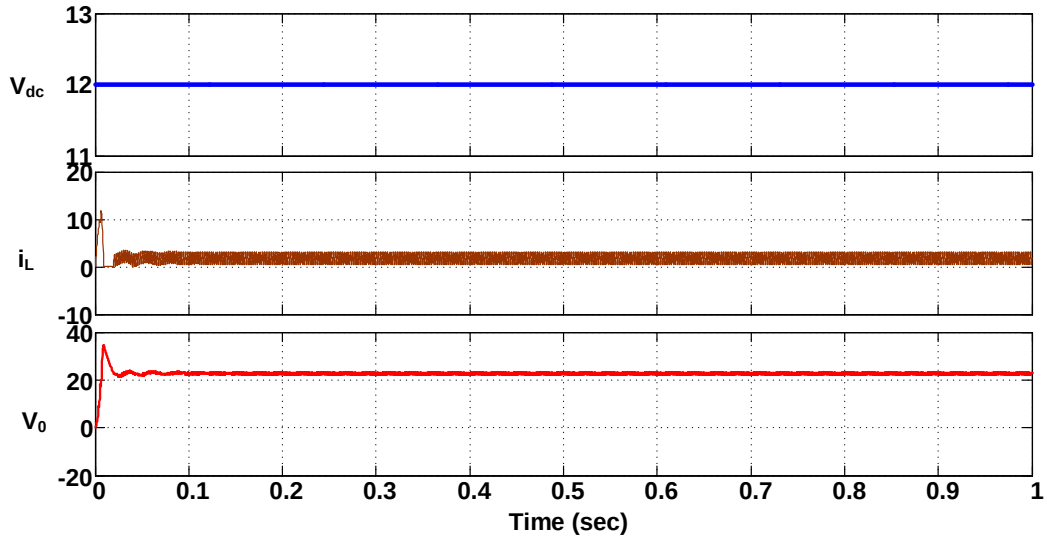


(b)

Fig. 4. Steady-state performance of the boost converter: Input voltage, Inductor current, and Output voltage (a) For a $V_0$ ref of 20 V, (b) For a $V_0$ ref of 24 V.

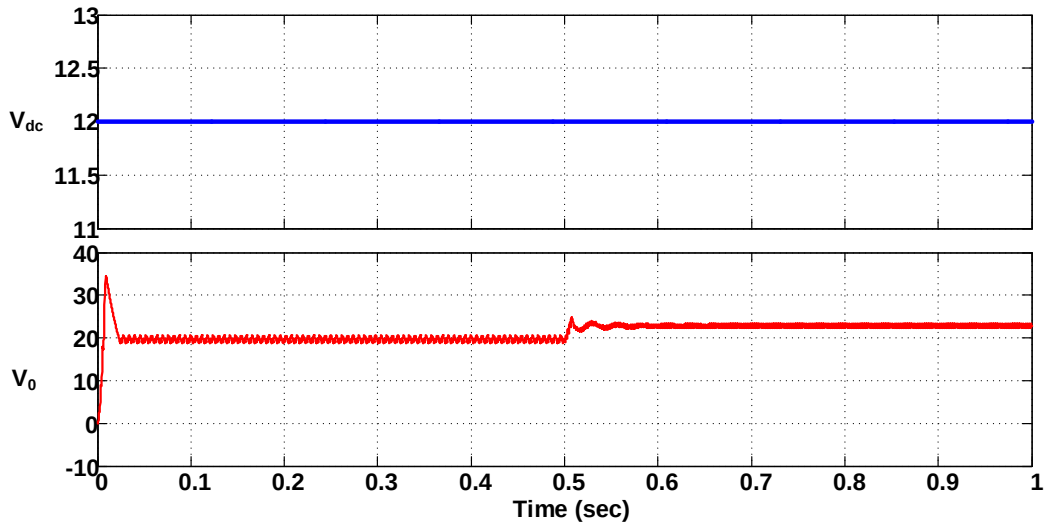


Fig. 5. Dynamic performance of the boost converter: Input voltage, and Output voltage for a step-change in $V_0$ ref from 20 V to 24 V.

## 5. Conclusion

This paper provides a comprehensive analysis of the operating modes of the boost converter and its closed-loop control technique. The proposed method is evaluated in both steady-state and transient states. The satisfactory results shows that the proposed method can be applied in several areas where control of output voltage is necessarily required. The proposed method requires fine tuning of P-I controller and a well-shaped hysteresis band. The frequency of switching can be controlled by altering the frequency of the carrier wave. Hence, the simulation results for the proposed method are presented using MATLAB/SIMULINK models.

## REFERENCES

[1] Rahman, S., & Lee, F. C. (1982). Computer simulations of optimum boost and buck-boost converters. *IEEE Transactions on Aerospace and Electronic Systems*, (5), 598-608.

[2] Szuba, S. (1980). An approach to the design of energy storage reactors for DC-to-DC switching power converters using ferrite structures. *IEEE Transactions on Magnetics*, *16*(5), 1271-1278.

[3] Chetty, P. R. K. (1982). Cieca: Application to current programmed switching DC-DC converters. *IEEE Transactions on Aerospace and Electronic Systems*, (5), 538-544.

[4] Matsuo, H., & Kurokawa, F. (1984). New solar cell power supply system using a boost type bidirectinal dc-dc converter. *IEEE transactions on Industrial Electronics*, (1), 51-55.

[5] Rim, C. T., Joung, G. B., & Cho, G. H. (1991). Practical switch based state-space modeling of DC-DC converters with all parasitics. *IEEE transactions on power electronics*, *6*(4), 611-617.

[6] T. Abhilash, A. Kirubakaran, and V. T. Somasekhar, "A Seven-Level VSI with a Front-end Cascaded Three-Level Inverter and Flying Capacitor fed H-Bridge", *IEEE Trans. Ind. Appl.*, vol. 55, no. 6, pp. 6073-6088, 2019.

[7] Wang, B., Zhang, X., & Gooi, H. B. (2018). An SI-MISO boost converter with deadbeat-based control for electric vehicle applications. *IEEE Transactions on Vehicular Technology*, *67*(10), 9223-9232.

[8] Wai, R. J., Lin, C. Y., Duan, R. Y., & Chang, Y. R. (2007). High-efficiency DC-DC converter with high voltage gain and reduced switch stress. *IEEE Transactions on Industrial Electronics*, *54*(1), 354-364.

[9] Restrepo, C., Calvente, J., Cid-Pastor, A., El Aroudi, A., & Giral, R. (2011). A noninverting buck–boost dc–dc switching converter with high efficiency and wide bandwidth. *IEEE Transactions on Power Electronics*, *26*(9), 2490-2503.

[10] Kruse, K., Elbo, M., & Zhang, Z. (2017, March). GaN-based high efficiency bidirectional DC-DC converter with 10 MHz switching frequency. In *2017 IEEE Applied Power Electronics Conference and Exposition (APEC)* (pp. 273-278). IEEE.